CIRCLE DETECTION USING THE IMAGE RAY TRANSFORM
A Novel Technique for Using a Ray Analogy to Extract Circular Features

Alastair H. Cummings, Mark S. Nixon, John N. Carter
School of Electronics and Computer Science, University of Southampton, Southampton, UK
ahc08r@ecs.soton.ac.uk, msn@ecs.soton.ac.uk, jnc@ecs.soton.ac.uk

Keywords: feature extraction image processing analogy ray-tracing wave light ray transform circle detection

Abstract: Physical analogies are an exciting paradigm for creating techniques for image feature extraction. A transform using an analogy to light rays has been developed for the detection of circular and tubular features. It uses a 2D ray tracing algorithm to follow rays through an image, interacting at a low level, to emphasise higher level features. It has been empirically tested as a pre-processor to aid circle detection with the Hough Transform and has been shown to provide a clear improvement over standard techniques. The transform was also used on natural images and we show its ability to highlight circles even in complex scenes. We also show the flexibility available to the technique through adjustment of parameters.

1 INTRODUCTION

Physical analogies are an exciting paradigm in computer vision that enable the creation of novel techniques that approach the problems of feature extraction from entirely different angles (Nixon et al., 2009). These analogy based techniques have the advantage of being based on physical properties of natural phenomena such as water, heat or force fields and so are more easily understood by those using them. In addition to the intuitive nature of the algorithms the parameters that are used have meanings that are clear and have real word analogues. Although analogy operators are heavily based upon a well defined physical concept, the analogies can be adapted outside this definition to increase their effectiveness and flexibility whilst maintaining the strengths provided by the analogy. These properties are a clear advantage over many standard techniques for which the mechanics can be hard to grasp and parameter selection is not clear.

Heat flow has been used a number of times due to its smoothing properties. Anisotropic diffusion (Perona and Malik, 1990) is an edge-aware smoothing technique that allows heat to flow across areas of low but not high edge strength, so preserving the important edge features whilst reducing noise. Direkoglu and Nixon developed two techniques using a heat flow analogy for finding moving edges and image segmentation. The first (Direkoglu and Nixon, 2006) used anisotropic diffusion to smooth images and then heat flow in the temporal dimension for extraction. The second (Direkoglu and Nixon, 2007) used heat flow to segment the image into non-contiguous sections and then used geometric heat flow to smooth the boundaries. This segmentation technique produced encouraging results which capitalised on the use of analogies.

Hurley's force field transform (Hurley et al., 2005) generates a force field from an image that is analogous to a gravitational or magnetic field. Each pixel is assumed to attract every other pixel with a force dependent on its intensity and the inverse square law. The sum of these forces generates a vector field representing an image. This force field can help in feature extraction and was successfully utilized to create an ear biometric. Xie et al. (Xie and Mirmehdi, 2008) also used a force field analogy, generated from magenetostatic theory and joined with an active contour model to enable contour detection. In their model the image border and evolving contour are assumed to have an electric current running through them and the interaction of these currents generates a force field. This field guides the development of the contour, changing

along with it to guide it to the image border.

This paper describes the creation of a novel transform based on using an analogy to rays of light. The rules of ray reflection and refraction are employed to enhance tubular and circular features within an image. The physical rules governing rays are described in section 2.1 whilst section 2.2 introduces the image ray transform. Section 3 documents empirical tests on circle detection with the ray transform in a variety of situations including examples of transformed natural images and section 4 draws conclusions and discusses the future direction of this research.

2 IMAGE RAY TRANSFORM

The image ray transform is a novel technique for extracting tubular and circular features that are not often found by other techniques. It uses a pixel based ray tracing technique and a subset of the laws of optics to trace rays through an image which then react to certain structural features to emphasise them. Whilst the transform is based on the principles of optics, the details of the technique can be adjusted to suit successful feature extraction rather than accurate simulation of the natural phenomenon. The implementation capitalises only on the basis of the analogy; we do not simulate intricate details of light propagation.

2.1 Laws of Optics

Rays are a method of modelling the propagation of waves, most often light, with specific regard for the direction of the wave as it interacts with its environment. Light travels through a medium and the course of the light will be altered when it crosses the boundary with a different medium. Figure 1 shows how the light may react by reflecting, refracting, or splitting and doing both. Light crosses the boundary between the media at an angle of θ_i between the light direction and the normal of the boundary (the dotted line). If reflection occurs then the light reflects, with $\theta_l = \theta_i$. If refraction occurs the light refracts at an angle of θ_r to the normal where θ_r is calculated from the refractive indices of n_1 and n_2 of the media m_1 and m_2. Refractive indices are the ratio of the speed of light in a vacuum to the speed of light within the media, and in nature $1 \leq n \lessapprox 4$. The angle of the refracted light θ_r is found by Snell's Law as

$$\frac{\sin\theta_i}{\sin\theta_r} = \frac{n_2}{n_1} \tag{1}$$

If $n_1 < n_2$ then light bends towards the normal, so $\theta_r < \theta_i$. If $n_1 > n_2$ then light bends away from the normal as long as it is below the critical angle θ_c. This is

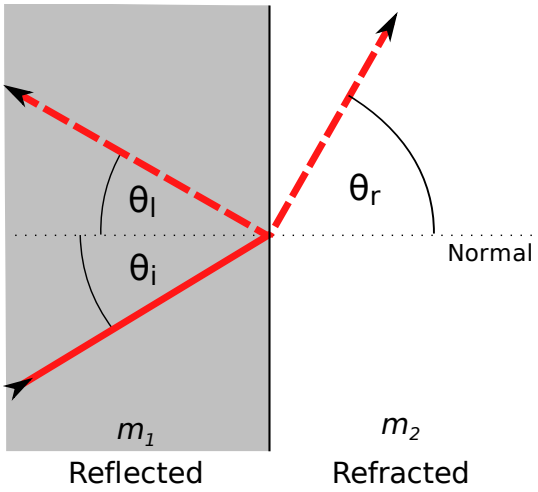

Figure 1: Refraction and reflection of light.

the angle for which θ_r would be greater than 90° and is therefore physically impossible and is calculated as

$$\theta_c = \sin^{-1}\left(\frac{n_2}{n_1}\right) \tag{2}$$

In this case the light is totally internally reflected in an identical manner to normal reflection. In the natural world the amount of refraction and reflection that occurs depends on the media and in most cases is a combination of the two, some part passing through, and some being reflected back. These rules form the basis of the image ray transform.

2.2 Image Ray Transform Mechanics

The image ray transform takes the laws of optics described previously and applies them to the problem of feature extraction.

2.2.1 Image Transform

The image ray transform works by tracing a number of rays through an image. The paths of these rays are then used generate a new image with tubular and circular features emphasised. The image is analogised to that of a set of two dimensional glass blocks, each representing a pixel whose refractive index is related to the intensity of the pixel in the image. One method to assign a refractive index to a pixel with intensity i is shown by equation 3 where $n_{\max}$ is a parameter that defines the maximum possible refractive index. The indices are then spaced evenly between 1 and $n_{\max}$.

$$n_i = 1 + \left(\frac{i}{255}\right) \cdot (n_{\max} - 1) \tag{3}$$

The splitting of rays into reflected and refracted parts is not considered.

In this matrix of blocks a ray is created with both the random position (x and y) and the direction (ϕ) drawn from a uniform distribution (U). For an image of size $w \times h$.

$$x \sim U[0,w), y \sim U[0,h), \phi \sim U[0,2\pi) \tag{4}$$

ϕ is converted into a unit vector, $\mathbf{V}$ representing the direction of the ray, as this easier to use in calculations, but cannot be generated from a uniform distribution.

$$\mathbf{V} = (\cos\phi, \sin\phi)^T \tag{5}$$

The ray function r traces the course of the ray and updates an accumulator $\mathbf{A}$. $\mathbf{I}$ is the image, from which refractive indices and the normals at each pixel are derived. d is the maximum number of reflections or refractions which the ray can undergo before tracing ceases, also known as the depth.

$$\mathbf{A}' = r(\mathbf{A}, \mathbf{I}, x, y, \mathbf{V}, d, n_{\max}) \tag{6}$$

The position vector $\mathbf{p}$ initialises the ray at

$$\mathbf{p}^{<0>} = (x,y)^T \tag{7}$$

and at iteration i,

$$\mathbf{p}^{<i+1>} = \mathbf{p}^{<i>} + \mathbf{V} \tag{8}$$

At each pixel through which the ray passes $\mathbf{A}$ is updated to show that the ray has passed through.

$$\mathbf{A}'(\mathbf{p}^{<i+1>}) = \mathbf{A}(\mathbf{p}^{<i+1>}) + 1 \tag{9}$$

$\mathbf{A}(\mathbf{p})$ is only increased once per ray, so as to prevent small loops in the ray's path repeatedly increasing a single pixel and excessively emphasising noise or other undesirable features. When crossing a pixel boundary where the media on either side are of differing refractive indices, a new path must be calculated using a vector formation of the laws described in section 2.1.

If $\mathbf{N}$ is the normal and n_1 and n_2 are the refractive indices of the first and second media then the angle of incidence θ_i can be found.

$$\cos\theta_i = \mathbf{N} \cdot \mathbf{V} \tag{10}$$

If $n_1 > n_2$ we have to test whether we should internally reflect or refract. The critical angle θ_c must be found from equation 2 and if $n_2 > n_1$ or $\theta_i < \theta_c$ and assigning $n = \frac{n_1}{n_2}$ then the direction of refraction R_r is, from (Hill, 2000),

$$\mathbf{R}_r = n\mathbf{V} + (n(\mathbf{N} \cdot \mathbf{V}) - \cos\theta_r)\mathbf{N} \tag{11}$$

where $\cos\theta_r$ is

$$\cos\theta_r = \sqrt{1 - n^2(1 - \mathbf{N} \cdot \mathbf{V})} \tag{12}$$

If $n_1 > n_2$ and $\theta_i > \theta_c$ then the ray totally internally reflects. The direction of reflection $\mathbf{R}_l$ is then

$$\mathbf{R}_l = \mathbf{V} - 2(\mathbf{N} \cdot \mathbf{V})\mathbf{N} \tag{13}$$

$\mathbf{R}_l$ or $\mathbf{R}_r$ are then assigned to $\mathbf{V}$

$$\mathbf{V}' = \begin{cases} \mathbf{R}_l \text{ if } n_1 > n_2 \wedge \theta_i > \theta_c \\ \mathbf{R}_r \text{ otherwise} \end{cases} \tag{14}$$

The ray is traced in this manner until it has either undergone d reflections or refractions or the ray exits the image. This is repeated for N rays and the accumulator gives the transformed image.

The values of the normals ($\mathbf{N}$) that are used to calculate the new directions of rays are always set to the normal of the edge direction found by the Sobel operator at that point. In figure 2 this normal is shown orthogonal to that of the edge direction $\mathbf{E}$, as well as the normals of the pixel boundaries $\mathbf{B}_1$ and $\mathbf{B}_2$. $\mathbf{N}$ is used rather than $\mathbf{B}_1$ or $\mathbf{B}_2$ as it is more representative of the information within the image. Currently we only perform refraction when moving from higher to lower refractive indices as this tends to improve the quality of the transform result, and we are working to improve this further.

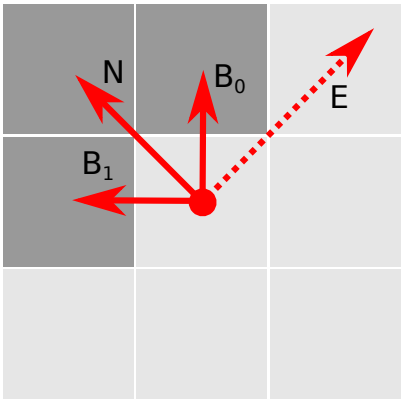

Figure 2: The normals that could be used to calculate reflections and refractions.

Figure 3 shows the path of a ray as it travels through a simple image. The edge direction at each pixel is horizontal, and hence the normal at each point is vertical. The ray is initialised at position A with a random direction and advances to position B. The intensity of the cells reflects their refractive index. At B the refractive indices of the current and next pixel are compared (n_1 and n_2 respectively), and as $n_1 = n_2$ the ray continues with no change in direction. At C, $n_1 < n_2$, and so the ray bends towards the normal, whilst at D $n_1 > n_2$ and so the ray bends away from normal. At E total internal reflection occurs, because

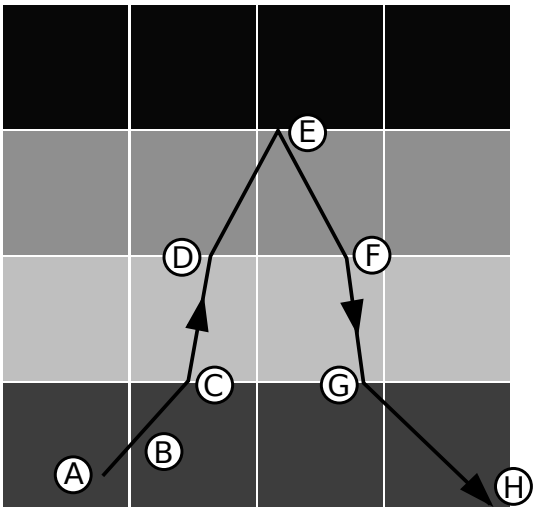

Figure 3: An example of the course a ray might take in a simple 4x4 image.

$n_1 > n_2$ and $\theta_i > \theta_c$. At F and G the occurrences at C and D are repeated in reverse order whilst at H the ray exits the image and the trace terminates.

2.2.2 Refinements

In addition to the basic transform, a number of additional parameters and processes can be performed with the transform to give a wider range of results and to extend the range of circumstances in which the transform is useful.

The transform will only extract features that have larger refractive indices than the surrounding area because total internal reflection only prevents rays from passing from materials with higher to lower refractive indices, and not vice versa. As the refractive index is proportional to intensity, this has the effect of extracting features that are lighter than their surrounding area. Depending on what is known about the properties of the features to be extracted different measures can be taken to overcome this problem.

If the approximate intensity of the desired features is known then the image can be easily transformed to make that intensity (the target intensity) have the highest value. This can be done by finding the difference from the target intensity t to the original intensity i_o for each pixel, as in equation 15.

$$i_t = 255 - |i_o - t| \tag{15}$$

If the expected intensity is not known then the ray transform can be performed multiple times, with different target intensities, and the highest value at each pixel used. This is shown in equation 16 where $\mathbf{I}$ is the final image and $\mathbf{I}_x$ are the results of different transforms with different target intensities.

$$\mathbf{I} = \max(\mathbf{I}_0, \mathbf{I}_1, \ldots, \mathbf{I}_x) \tag{16}$$

It may also be the case that the difference in intensity between features and the surrounding area are not significant enough to extract it with the linear refractive indices calculated by equation 3. In such a case an alternative version can be used (equation 17) that assigns refractive indices exponentially, to ensure greater difference, and more refraction and reflection.

$$n_i = e^{\frac{i}{k}} \tag{17}$$

In this case it is k rather than $n_{\max}$ that controls the scale of the refractive indices.

2.3 Transform Properties

The results of the transform show its ability to extract both tubular and circular features. In figure 4 some of the strengths of the ray transform are displayed. Whilst the box is weakly emphasised, both the curve and the circle are shown with greater intensity. The curve is extracted because it acts is if it were an optical fibre or tube, guiding the rays along it as they bounce of the walls because of total internal reflection. At either end of the curve a spread of rays can be seen, where they have exited the end of the tube at an angle at which total internal reflection cannot occur. The transform has treated the circle differently however, and given it a strong edge. Figure 5 shows how this occurs when rays repeatedly reflect off the edges of the circle at angles shallow enough to ensure that subsequent boundary collisions will also result in reflection. Across a large number of rays this creates a gradient around the edge of the circle.

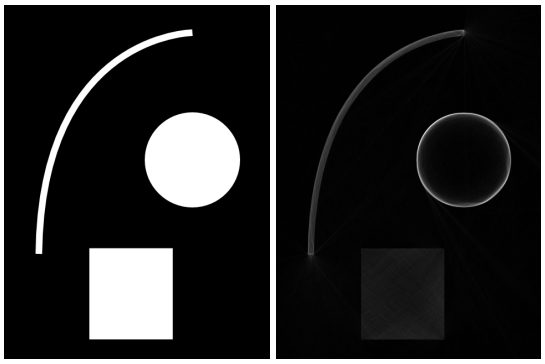

(a) Original (b) Ray Transform

Figure 4: Ray transform on a simple image. $N = 20000$. $d = 256$ and $n_{\max} = 3$.

An advantage of an analogy based operator is that parameters are intuitive and easily set. The ray transform has 3 main parameters, two of which affect

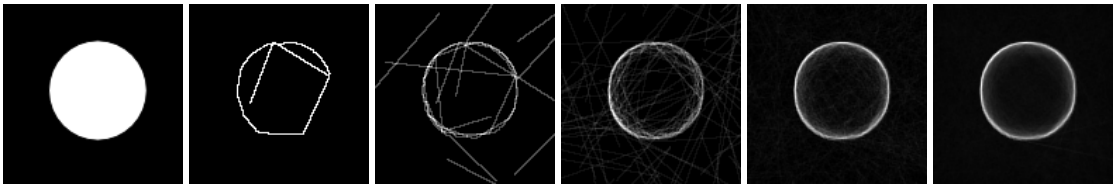

(a) Original (b) $N = 1$ (c) $N = 10$ (d) $N = 100$ (e) $N = 1000$ (f) $N = 10000$

Figure 5: Accumulator throughout ray transform on simple circle. $d = 128$ and $n_{\max} = 40$.

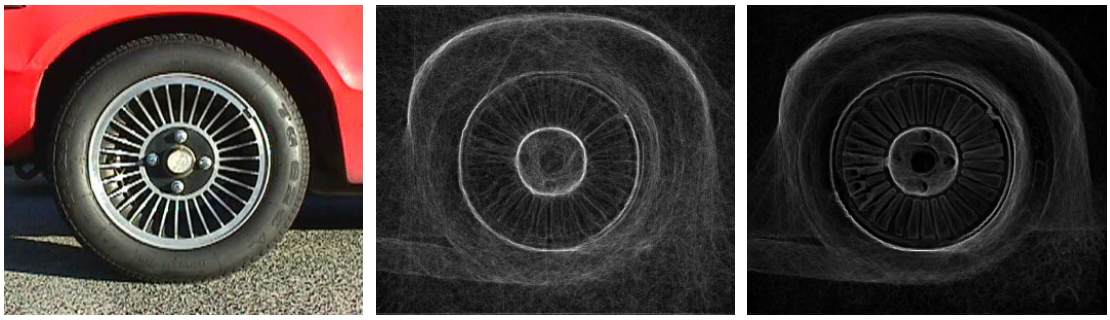

(a) Original (b) $n_{\max} = 1.5$ (c) $n_{\max} = 40$

Figure 6: Results of ray transform on variety of values of $n_{\max}$. $d = 256$, $N = 10000$ and $t = 0$.

smoothness. N, the number of rays traced, affects the smoothness of the resultant image, if it is too low there are not enough rays traced to cover the whole image, and if it is set too high will make the transform too slow. The number of reflections or refractions a ray is allowed to make before tracing is stopped, d, must be set large enough to allow rays to interact with important features, but must not be longer than necessary as the transform will be slowed. The influence of these parameters on the speed of the transform will be discussed below. The maximum refractive index, $n_{\max}$, and the target intensity, t, do not affect the speed of the transform but change the features that are extracted. As detailed above, t allows a selected intensity (or multiple intensities) to be focussed on but $n_{\max}$ has the greatest effect on the result. Figure 6 shows an image transformed with a range of refractive indices. By using a small value for $n_{\max}$ such as 1.5, only the strongest features are shown (the arch and tyre rims), whilst with larger, unnatural values many weaker features become strong (such as the individual tyre spokes).

Due to the non-deterministic nature of the transform, the image produced will sometimes contain noise. This can be dealt with either by increasing N to reduce the effect of the random ray initialisation, or by increasing the value of $n_{\max}$ to ensure rays conform more strongly to the image or by using additional smoothing.

The transform was implemented in Python with the bulk of the algorithm written as a C extension using F2PY (Peterson, 2009). Computation time depends on the parameters more than image dimensions, although image size drives their selection. For a 512x512 image with $N = 10000$ and $d = 256$ computation time was 1.53s. For comparison a 3x3 sobel operation took 0.13s on the same machine. The speed tests were done on a Core 2 Duo 2.53GHz, not using any form of parallel processing. Whilst significantly slower than Sobel, the time taken to compute the ray transform is not excessive. Memory requirements are not significant and the above test used approximately 50MB at peak usage. Setting $N = 20000$ increases computation time to 2.93s whilst setting $d = 512$ increases it to only 2.21s as not all rays will be traced to the full depth. A Java applet demonstration is available online at `http://users.ecs.soton.ac.uk/ahc08r/rt/`

3 CIRCLE DETECTION

Due to the unique way that the transform reacts to simple circles its effectiveness at aiding circle detection was investigated. The standard method of circle detection is the Hough transform (HT) for circles and the ray transform was used as a pre-processor to improve its performance. The HT was originally designed for detecting lines (Hough, 1962) but can be

applied to detection of arbitrary shapes. The standard version for circles operates on a binary edge image and generates an accumulator of position and, if unknown, circle radius. At each edge pixel in the image a circle around it is voted for in the accumulator, with the centre of the circle being the peak, and the votes at the peak coming from the points on the circumference. The transform can be extended to deal with an unknown radius by voting in a cone around the point, with each level in a 3D Hough space representing a differing radius. (Yuen et al., 1990) review a number of simple Hough transform variations and (Davies, 1984) describes the decomposed type used. This version was used because of its significantly greater speed than the standard transform. It has this property because the centre is discovered by voting in lines that are normal to the edge direction of the edge points in a 2D search space. Once the centre has been found the most likely radius was found in a fast 1D accumulator. Typically edge detection operators such as thresholded Sobel or Canny are used to create the binary edge image on which the Hough transform is performed. The ray transform highlights a circle in an image, but does not produce a single thin strong edge, so it must be used as a pre-processor in conjunction with a standard edge detection technique to create stronger, more distinct edges. Whilst there are more sophisticated and effective Hough Transforms and edge detection techniques available, these tests are designed to show that the ray transform can improve results independently of other methods used.

3.1 Simple Circles

To test the usefulness of the image ray transform for circle detection, a number of empirical tests were performed. Images were created by adding a number of circles onto a series of background images with complex features (figure 7). Images of the type shown in figure 7(c) had backgrounds randomly generated wherein the intensity of each pixel was drawn individually from a uniform distribution with interval $[0,255]$, whilst the other images had the same background for each test image. Every test image had a different, randomly generated circle placed upon it, and were then processed by the image ray transform. The parameters used were $N = 10000$, $n_{\max} = 40$, $d = 256$ and two passes were made with $t = \{0,255\}$ and combined by equation 16 so as to detect both light circles on backgrounds of both higher and lower intensity.

Each of these images was then tested with the decomposed Hough transform for circles and the distance from the actual position and radius was found

(a) Tree

(b) Sea

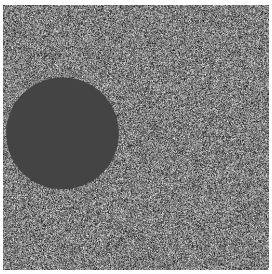

(c) Noisy

Figure 7: Examples of images generated on different backgrounds.

and used as the error.

$$E = \sqrt{(x-x_0)^2 + (y-y_0)^2 + (r-r_0)^2} \qquad (18)$$

Both the original images and the transformed versions had the Sobel and Canny operators applied to them and figure 8 shows the mean error across the Hough transforms of all images. The error bars represent the standard error of the distance between the prediction and correct values for the circle parameters. It is clear that the application of the ray transform to the images improves the performance significantly.

Both the Canny and Sobel operators depend on change in intensity to produce edges, and in the thresholding process weak edges will often be removed, and thus cannot contribute to the voting process in the Hough transform. The ray transform highlights structure, and so small intensity differences can be exaggerated to the point where they are far more significant. Figure 9 shows an original and ray transformed image having undergone the Sobel operator. Whilst the application of the ray transform introduces some noise within the circle, the edge around the circle is far stronger than any other edge in the image. This contrasts with the Sobel operator alone where the edges created by the background are of comparable strength to the edge surrounding the circle.

In images set on a background of random noise, use of the ray transform improves detection at all in-

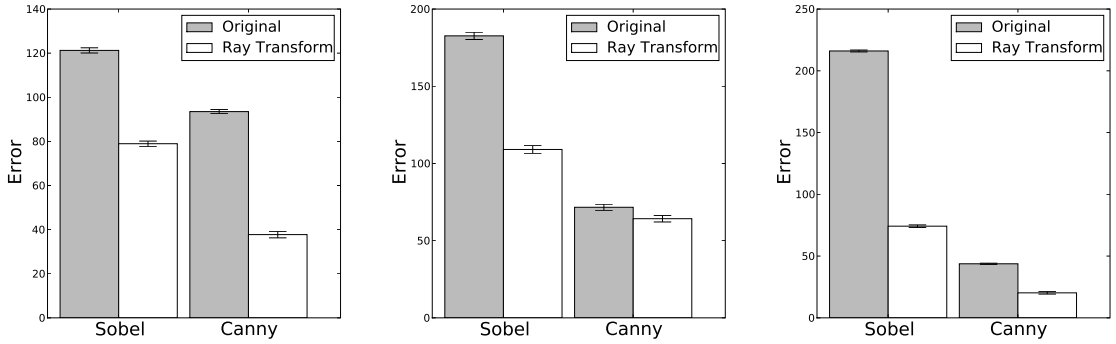

(a) Tree (b) Sea (c) Noisy

Figure 8: Mean error for circle detection on different background images.

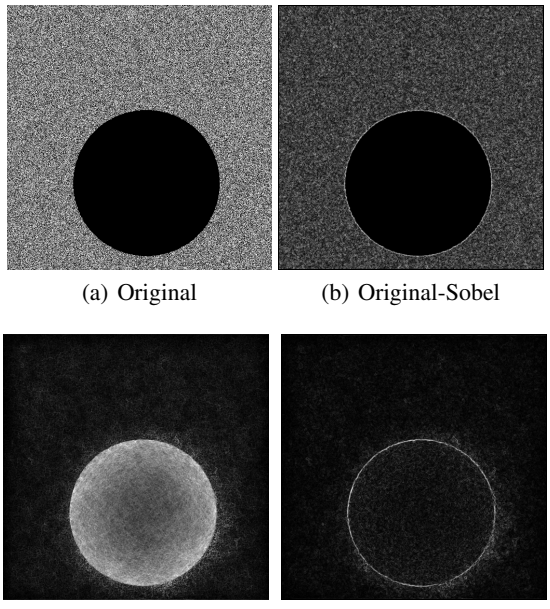

(a) Original (b) Original-Sobel

(c) Ray Transform (d) Ray Transform-Sobel

Figure 9: The results of a single image after the application range of techniques.

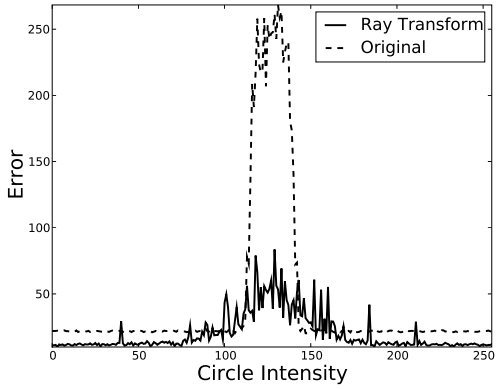

Figure 10: Error across circle intensities for Canny HT tests with a noisy background

tensities of circle, but has a more significant effect in cases where there is very little difference in intensity between circle and background (figure 10). With the Canny operator and a noisy background, both the ray transformed image and the original image perform well on most circle intensities. The ray transform is generally more accurate because it does not need such a high level of smoothing to reduce the strength of the background noise, and so the found coordinates are not displaced by as great an amount. The increase in error in the detection in both cases coincides with the intensity of the circle being close to the mean intensity of the background. The ray transformed images achieve significantly better results than the original images in these cases however, as the results for the original images suggest that no circle was found in any case, whilst in the ray transform the correct circle was found in most cases.

The application of the ray transform to an edge image is another method through which circle detection might be enhanced. As the ray transform is capable of extracting tubular features, converting an image into a series of tubes through an edge detection operator is a possible approach to increasing the efficacy of the transform. In figure 11 are the results of the application of the ray transform to some of the generated images where the refractive indices were found from the Sobel edge magnitude. In figures 11(a) and 11(c) the circle of high intensity has edges that are extracted clearly, but the circle of medium intensity in figures 11(d) and 11(f) is not emphasised as much due to the reduced contrast with the surrounding image. These results suggest that whilst use of the transform on an edge image could be appropriate in some situations, it is not for circle detection as it does nothing to emphasise edges of circles over the rest of the image as the intensity ray transform does.

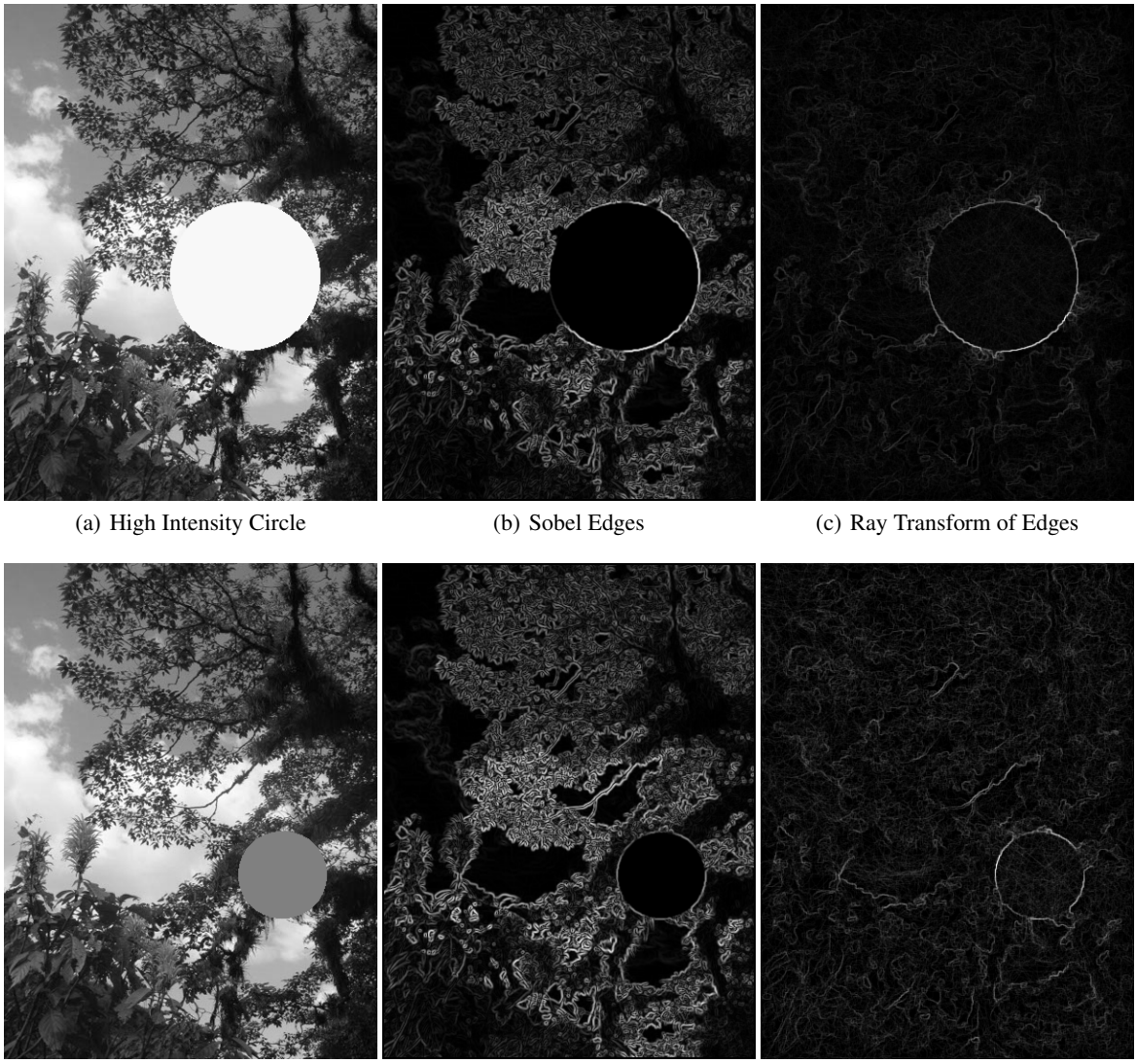

(a) High Intensity Circle (b) Sobel Edges (c) Ray Transform of Edges

(d) Medium Intensity circle (e) Sobel Edges (f) Ray Transform of Edges

Figure 11: The results of the ray transform on the Sobel edge images of some circles. $N = 10000, n_{\max} = 40, d = 64$.

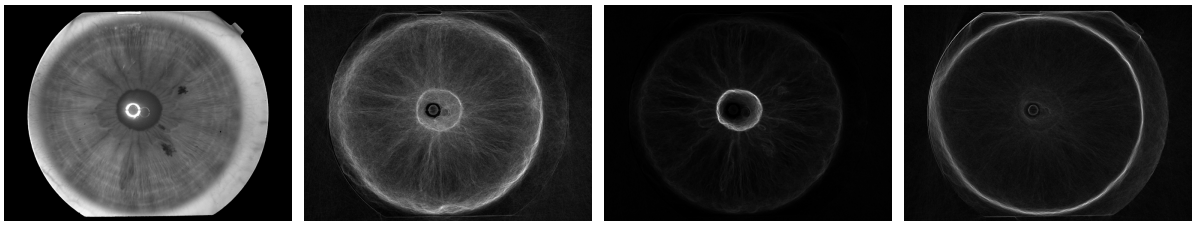

(a) Original (b) $t = 40$ (c) $t = 0, k = 50$ (d) $t = 128, n_{\max} = 2$

Figure 12: Ray transform of an iris image, with differing parameters extracting different areas. Unless otherwise stated parameters are $N = 40000, d = 512, n_{\max} = 40$ or not used.

3.2 Natural Images

The transform was also tested on some real images. Whilst we continue to search for a standard circle detection database, some natural images of circles were tested to see the results of the ray transform. In figure 12 the results of a number of transforms on an image of an iris are shown. By varying the parameters used, different circles that are present in the eye can be highlighted. In figure 12(b) the two strongest circles, around the pupil and the iris are extracted whilst figures 12(c) and 12(d) show each individual circle being extracted far more strongly.

The transform was also tested on images of a bicycle (figure 13) from the Wiry Object Recognition Database (WORD) (Carmichael and Hebert, 2004). The transform is able to highlight the circular wheels very strongly, with many other background features disappearing. Examining the thresholded version of the image in figure 13(c) it is also clear that tubular features such as the bag's strap and horizontal mortar in the wall act as tubular features and so are extracted strongly.

(a) Original

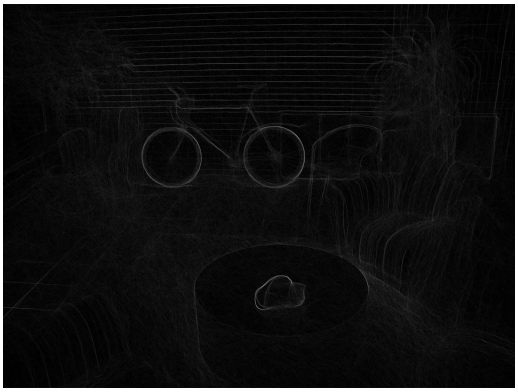

(b) Ray transform

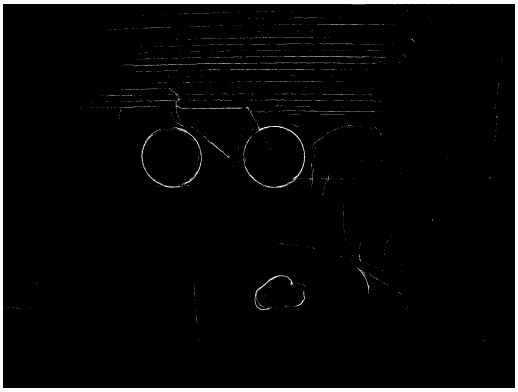

(c) Thresholded

Figure 13: Ray transform of a bicycle from WORD. $N = 20000, d = 256, n_{\max} = 4$. Threshold parameter was 50.

4 CONCLUSIONS AND FURTHER WORK

We have created a novel transform that is able to extract circular and tubular features from images. We have shown that it can act as a pre-processor for circle detection and significantly improve results with different techniques, even on hard cases where there is little intensity difference between the circle and background. The transform has also been shown to work with natural images, and it is flexible enough to extract individual or all circles within an image.

Whilst this work has focussed on the transform's ability to extract circles, it is also strong at emphasising tubular features and future work will concentrate on some of these. Some examples of possible areas are veins and rivers as well as some biometric applications such as ears and gait. The transform could also be expanded into 3D, with either 3D images, or video in a spatio-temporal format to track objects.

REFERENCES

Carmichael, O. and Hebert, M. (2004). Word: Wiry object recognition database. rope.ucdavis.edu/~owenc/word.htm. Carnegie Mellon University.

Davies, E. R. (1984). A modified Hough scheme for general circle location. *Pattern Recognition Letters*, 7(1):37–43.

Direkoglu, C. and Nixon, M. S. (2006). Low level moving-feature extraction via heat flow analogy. *Lecture Notes in Computer Science*, 4291:243–252.

Direkoglu, C. and Nixon, M. S. (2007). Shape extraction via heat flow analogy. *Lecture Notes in Computer Science*, 4678:553–564.

Hill, F. (2000). *Computer graphics using OpenGL*. Prentice Hall, 3rd edition.

Hough, P. (1962). Method and means for recognizing complex patterns. U.S. Patent 3.069.654.

Hurley, D. J., Nixon, M. S., and Carter, J. N. (2005). Force field feature extraction for ear biometrics. *Computer Vision and Image Understanding*, 98:491–512.

Nixon, M. S., Liu, X. U., Direkoglu, C., and Hurley, D. J. (2009). On using physical analogies for feature and shape extraction in computer vision. *The Computer Journal*.

Perona, P. and Malik, J. (1990). Scale-space and edge detection using anisotropic diffusion. *IEEE Transactions on Pattern Analysis and Machine Intelligence*, 12(7):629–639.

Peterson, P. (2009). F2PY: a tool for connecting fortran and python programs. *International Journal of Computational Science and Engineering*, 4(4):296–305.

Xie, X. and Mirmehdi, M. (2008). MAC: Magnetostatic active contour model. *IEEE Transactions on Pattern Analysis and Machine Intelligence*, 30(4):632.

Yuen, H., Princen, J., Illingworth, J., and Kittler, J. (1990). Comparative study of Hough transform methods for circle finding. *Image and Vision Computing*, 8(1):71–77.